Journal of Material Cycles and Waste Management (2020) 22:1867–1876
https://doi.org/10.1007/s10163-020-01083-6

ORIGINAL ARTICLE

Self-recycling of sewage sludge as a coagulant and mechanism in sewage sludge dewatering

Jiahuan Wu[1,2,3,4,5] · Tao Lu[1,2,3] · Guang Yang[5] · Wei Meng[5] · Haoran Yuan[1,2,3] · Yong Chen[1,2,3]

Received: 19 February 2019 / Accepted: 24 June 2020 / Published online: 22 September 2020

Abstract

The properties of sewage sludge-derived biochar (BC) pyrolyzed at 300–900 °C were characterized, and which exhibited the basic properties of coagulant. When 1 g BC500 was added to 100 mL waste-activated sludge (WAS), the maximum mean settlement rate reached 8.20 mL min^{-1} within 10 min, and the volume of the settlement with settling time decreased to 13 mL. The capillary suction time of BC500 (12 s) was superior to those of municipal solid waste incineration (MSWI) fly ash (13.40 s), coal fly ash (14.20 s), and activated carbon (12.20 s). In addition, added BC may reduce the moisture content of sludge cake, especially for BC500. It can be that soluble cations and organic functional groups neutralize the negative charge of WAS which is helpful to shorten settling time. Meanwhile, the pore structure is beneficial for reducing moisture content of sludge cake. As results shown, BC was feasible to improve sewage sludge dewatering used as a coagulant.

Keywords Biochar · Characteristics · Coagulant · Pyrolysis · Sewage sludge

Abbreviation

V Volume of the settlement with settling time

Introduction

Sewage sludge is highly heterogeneous, and contains both organic and inorganic matters [1]. Because of the high organic matter content (38.40 ± 12.70%), sewage sludge should not be reconsidered as waste, but rather as a raw energy resources or other biodegradable materials [2–6]. Dewatering is a key step for sludge resource disposal, further energy and resource utilization [7]. Flocculants or coagulants are widely used to treat wastewater and enhance sludge dewaterability for a long time [8, 9]. However, traditional inorganic flocculants and synthetic polymeric flocculants produced from oil-based products may cause potential secondary pollution. For instance, some coagulant aids (e.g., fly ash, rice husk, lignite, and coal fly ash) have recently been investigated in detail. Hwa and Jeyaseelan [6] adopted fly ash as a skeleton builder, and found that the specific resistances and suction times of oily sludge decreased rapidly when 3% fly ash were amended. Meanwhile, Wu et al. [7] showed that biochar (pyrolyzed from mixture of sludge, ferric salt, and rice husk) prepared at 400 °C led to 63.90% decrease of sludge specific resistance and 39.20% increase of net sludge solid yield. Thapa et al. [8] concluded that the dewatering rate of sludge increased 5 times when lignite conditioning in conjunction with polyelectrolyte flocculation compared to the polyelectrolyte flocculation alone. Chen et al. [9] chose coal fly ash modified with sulfuric acid as a skeleton builder, and the results showed that the specific resistance to filtration of the sludge decreased from 1.86×10^{13} to 4.23×10^{11} m kg^{-1}, while the filter cake moisture content decreased from 86.90 to 56.52%. Compared to common coagulant aids, such as fly ash, rice husk, lignite,

Electronic supplementary material The online version of this article (https://doi.org/10.1007/s10163-020-01083-6) contains supplementary material, which is available to authorized users.

✉ Haoran Yuan
yuanhr@ms.giec.ac.cn

1 Guangzhou Institute of Energy Conversion, Chinese Academy of Sciences, Guangzhou 510640, People's Republic of China

2 CAS Key Laboratory of Renewable Energy, Guangzhou 510640, People's Republic of China

3 Guangdong Provincial Key Laboratory of New and Renewable Energy Research and Development, Guangzhou 510640, People's Republic of China

4 University of Chinese Academy of Sciences, Beijing 100049, People's Republic of China

5 Shenzhen Gas Corporation Ltd., Shenzhen 518049, People's Republic of China

and coal fly ash used in these researches, one obvious advantage of BC is it does not increase the complexity of sewage sludge composition, which will contribute to subsequent sewage sludge disposal and utilization.

In this study, the characteristics of sewage sludge-derived BC produced at different temperatures were examined. The dewatering effects of BCs, MSWI fly ash, coal fly ash, and activated carbon on waste-activated sludge (WAS) were compared using the settling test, capillary suction time (CST), sludge cake moisture content, and dewatering rate. The possibility of improving sewage sludge dewaterability with BC as coagulant was studied. Finally, the mechanism of BC on sludge dewaterability was analyzed.

Experimental

Materials

Sewage sludge and WAS were collected from the Yanbu municipal wastewater treatment plant (Foshan, China; 23°7′50″N, 113°10′46″E). Dewatered sludge was oven-dried at 105 °C until a constant weight and then crushed with a grinder at room temperature, after which it was reserved in an airtight plastic bag. Sewage sludge samples were pyrolyzed in a horizontal quartz reactor (Fig. 1) at 300, 500, 700, and 900 °C under a N_2 flow at 120 mL min^{-1} [10, 11]. The heating rate was 10 °C min^{-1}, and the holding time was 4 h. Sewage sludge samples pyrolyzed at 300, 500, 700 and 900 °C were denoted as BC300, BC500, BC700, and BC900, respectively. Meanwhile, we adopted boric acid solution (0.2 mol L^{-1}) and sodium hydroxide solution (0.2 mol L^{-1}) as tail gas absorber, and anhydrous calcium chloride as gas dryer.

MSWI fly ash was obtained from waste incineration plant (Likeng, Guangzhou, China), coal fly ash was purchased from Henan Sitong Chemical Construction Co., Ltd., and activated carbon was purchased from Shanghai Macklin biochemical technology co., LTD.

Proximate analysis

The sewage sludge sample was dried in an oven at 105 °C until a constant weight. And then the moisture content of sludge cake was calculated by mass change. The ash and volatile matter contents were tested using a muffle [12]. The ash content was determined as the weight loss at 815 °C for 1 h, and the volatile matter content was acquired by the weight loss when dried sample was heated in muffle at 900 °C for 7 min [13, 14]. Fixed carbon was calculated via the subtraction method. The results of the proximate analysis are shown in Table 1.

Biochar characterization methods

Biochar yield

We calculated the BC yield (BY) using Eq. (1) [12]:

$$BY(\%) = (WBC/WDS) \times 100\% \quad (1)$$

where WBC is the weight of BC and WDS is the weight of the dry sewage sludge sample before pyrolysis.

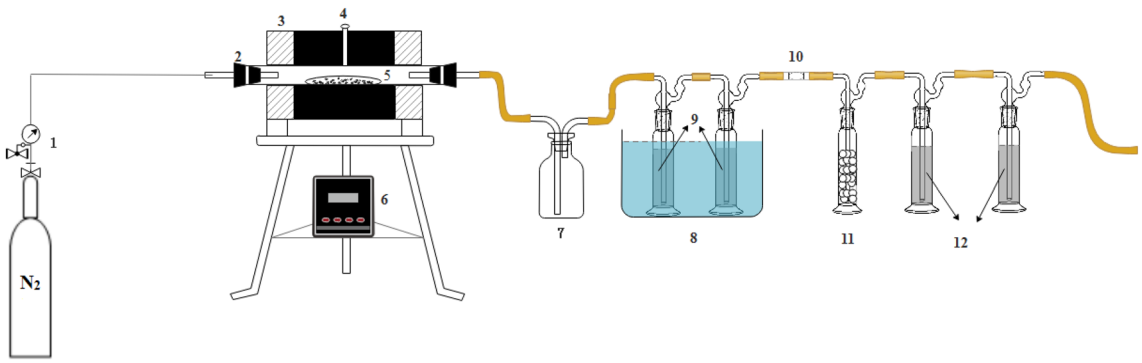

Fig. 1 A schematic of the experimental system: 1-flowmeter, 2-rubber plug, 3-horizontal tubular quartz reactor, 4-thermocouple, 5-ceramic boat, 6-temperature controller, 7-gas bottle, 8-shaker incubator, 9,12-tail gas absorber, 10-cotton filter, 11-anhydrous calcium chloride

Table 1 The proximate analysis and ultimate analysis of sewage sludge

Parameter	Proximate analysis				Ultimate analysis				Zeta potential of WAS (mv)
	Moisture	Ash[a]	Volatile matter[a]	Fixed carbon	C	H	N	S	
Value (%)	78.80	63.24	33.50	3.26	16.01	3.02	2.53	0.88	− 14.5

Biochar pH

First, 2.5 g BC sample was dispersed into 50 mL ultrapure water, and then the liquid was heated and stirred to a boil under air tight conditions with a magnetic heated stirrer for 5 min. When filtering, 5 mL aliquots of the primary filtrate were discarded [15]. The subsequent filtrate was tested with a portable pH meter (Ph-10/100; Bonsai Instrument Technology Co. Ltd., Shanghai, China) at room temperature.

Scanning electron microscopy

The surface structure of BC was studied using scanning electron microscopy (SEM; S-4800; Hitachi, Tokyo, Japan). SEM images of BC samples were obtained with an accelerating voltage of 2.0 kV in high-vacuum mode [3, 12, 16].

Elemental composition

The elemental composition of carbon, hydrogen, nitrogen and sulfur of the raw sewage sludge and BC samples were determined using an elemental analyzer (vario EL cube; Elementar Analysensysteme GmbH, Langenselbold, Germany) via flush combustion at 1020 °C using 5 mg each sample. Meanwhile, X-ray fluorescence analysis (XRF; AxiosmAX-Petro; PANalytical B.V., Netherlands) was used to identify metals in the samples from oxygen and uranium under normal operating conditions of 160 mA current input and 4 kW full power excitation [17].

Zeta potential

The zeta potential of BC was measured using a Zeta-master potentiometer (Mastersizer 2000E; Malvern Instruments, UK). First, 0.5 g each BC sample was added to 50 mL deionized water, and the solution was mixed using an ultrasonic cleaning machine.

Nitrogen adsorption

Nitrogen adsorption isotherm data were obtained at 77 K using an automatic station-type physical adsorption instrument (SI-MP-10; Quantachrome, Boynton Beach, FL, USA). Before the experiment, the samples were degassed at 120 °C for 24 h. Based on the isotherms, surface area (BET method), total pore volume, V_t (the point selected at the value of $p/p0 \sim 0.99$), volume of mesopores and volume of macropores (i.e., difference between the total pore volume and mesopore volume) were calculated. The pore size distribution was calculated using the BJH method [17, 18].

Fourier-transform infrared spectroscopy

The functional groups on the BC samples were identified using Fourier-transform infrared spectroscopy (FTIR; TENSOR27; Bruker, Germany). Prior to FTIR analysis, BC and potassium bromide was dried at 105 °C for 12 h. The resulting spectra were the average of 61 scans, which were used to identify the functional groups based on their characteristic absorbance peaks. The spectra were obtained in range of 500–4000 cm^{-1} with a resolution of 0.4 cm^{-1}, and the accuracy of the wave number was 0.005 cm^{-1}.

X-ray photoelectron spectroscopy

Element types, chemical valence, and relative contents were analyzed using X-ray photoelectron spectroscopy (XPS; ESCALAB 250Xi; Thermo Fisher Scientific Inc., Waltham, MA, USA). The X-ray source was operated at 150 W with an energy of 1486.68 eV, a spot size diameter of 500 μm, an electron takeoff angle of 90°, and monochromatic Al (Kα) radiation. The spectra were recorded with a concentric hemispherical analyzer in the constant-pass energy mode at 30 eV with a step size of 0.1 eV. The XPS spectra of the tested samples were analyzed using ThermoAvantage software (Thermo Fisher Scientific Inc.). Before the analysis, the binding energies were calibrated by adopting the following rules: C1s (284.8 eV) correction, 70% Gaussian/30% Lorentzian, and Shirley-type background subtraction.

Thermal analysis

A thermal analyzer (STA PT1600 TG-DSC; TA Instruments, Linseis, Germany) was used to analyze the thermos dynamic properties of sewage sludge under a N_2 atmosphere using the following program: heating rate of 5 °C min^{-1} from room temperature to 50 °C, maintenance for 30 min at 50 °C, and then heating at 10 °C min^{-1} to 100 °C; and a carrier gas (N_2) flow rate of 100 mL min^{-1}. The differential thermos gravimetric curves (DTG) were derived from TG curves.

Evaluation of sludge dewaterability

Sludge dewaterability was evaluated by the settling test, CST [19], and sludge cake moisture content. The WAS had with a water content of 99.8%.

First, 100 mL WAS was added to a beaker with a working volume of 200 mL, and 1 g BC was added and then stirred at 300 r min^{-1} for 2 min, followed by 120 r min^{-1} for 5 min, with an automatic agitator. The sludge was transferred to a 100 mL graduated cylinder after mixing. The volume of the

Table 2 Mean yield values of biochars produced at different pyrolysis temperatures

Pyrolysis temperature (°C)	Yield[a] (%)	pH[b]
300	81.97	6.10
500	70.30	7.50
700	68.32	8.12
900	63.91	8.29

[a]Based on dried basis

[b]Mean of three replicates

settlement with the settling time was recorded every 2 min under the effect of gravity for 30 min [20]. The volume of the settlement with settling time (V) was used as an index of the sludge settling rate. A smaller V value indicated a better settling effect. CST was tested using a capillary suction timer (Hangzhou Dedlfine Science & Technology Co. Ltd., Hangzhou, China). The sample was over-dried at 105 °C to a constant weight, and then cooled it to room temperature in desiccator. The moisture content was calculated by weight loss [21].

Results and discussion

Biochar yield, pH, and thermal analysis

The BY produced at different pyrolysis temperatures is shown in Table 2. The BY of BC300 was 81.97%. By contrast, at 500, 700, and 900 °C, the BY decreased to 70.30, 68.32, and 63.91%, respectively. Municipal sewage sludge has a highly complex composition. Thus, the decrease in BY could be attributed to a steady increase in the degree of pyrolysis conversion (see Fig. 1) [15]. Moreover, under relatively lower geothermal conditions, the main influencing factors were evaporation of different types of moisture and thermal instability depending on the composition [22]. At higher temperatures, stable matter decomposition and secondary reactions were related to the reduction in BY [23]. According to previous reports, yield decreased significantly with increasing pyrolysis temperature [1, 4, 5], which is in agreement with our findings.

As was commonly observed for BC derived from both sewage sludge and other feedstock, an increase in temperature led to an augmentation in pH [24]. The pH values of BC300 were around 6.0. Analogously, at temperatures of 500 °C or higher than 500 °C, BC was weakly alkaline. At lower temperatures, BC may contain greater amount of acidic functional groups (e.g., phenolic and carboxylic groups) [17]. With increasing temperature, alkali metal salts were separated from the organic matrix, which increased the pH of BC. In addition, the effect of dewatering of the

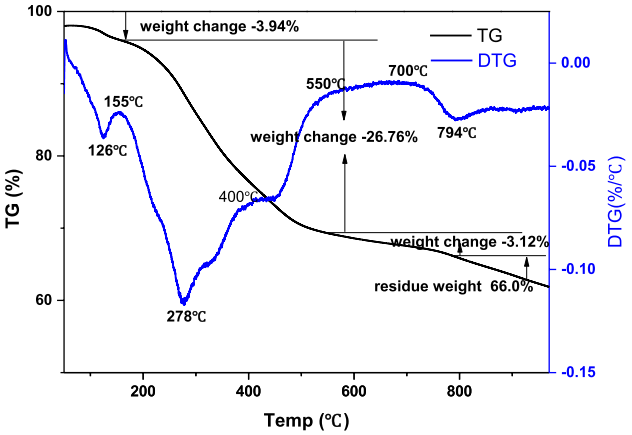

Fig. 2 TG and DTG curves for the dried sewage sludge during pyrolysis

feedstock was associated with a decrease in the amount of acidic surface groups during thermal treatment [24].

In the TG-DTG curves presented in Fig. 2, three distinct regions were identified, which were mainly related to BC yield. The initial weight loss of 3.94% from 50 to 155 °C was related to the water loss [25]. The second weight loss region occurred in the range of 155–550 °C, when 26.76% of the weight of sewage sludge was lost. This stage could be roughly divided into two sub-phases. At the temperature range of 155–400 °C, weight loss was result of decomposition of biodegradable organic matter (e.g., proteins and carboxyl groups), which resulted in the losses of mass caused by volatile analysis and by the combined evaporation of moisture [26, 27]. Thus, sludge volatilization could be carried out in a low-temperature zone. The second sub-phase occurred just before and up to 550 °C, which represented the delayed volatilization stage of high-boiling-point macromolecular organic compounds (e.g., aromatic rings, *N*-alkyl long-chain structures, and some saturated aliphatic chains) [27]. Overall, the majority of weight loss occurred in the second phase, because sewage sludge pyrolysis mainly occurred between 200 and 550 °C [1]. Finally, the third weight loss region occurred in the range of 550–860 °C, when the sewage sludge sample showed a 3.12% weight loss, and slowly approaching a final residue weight of 66%. This process was related to decomposition of carbonates, such as calcium carbonate, sodium carbonate, potassium carbonate, potassium chloride, and magnesium carbonate [2]. This period was marked by an approximate constant rate of weight loss.

SEM, elemental composition, XPS, and zeta potential

The pore structure of BC is beneficial for sludge dewatering as a skeleton builder. Under high pressure during mechanical

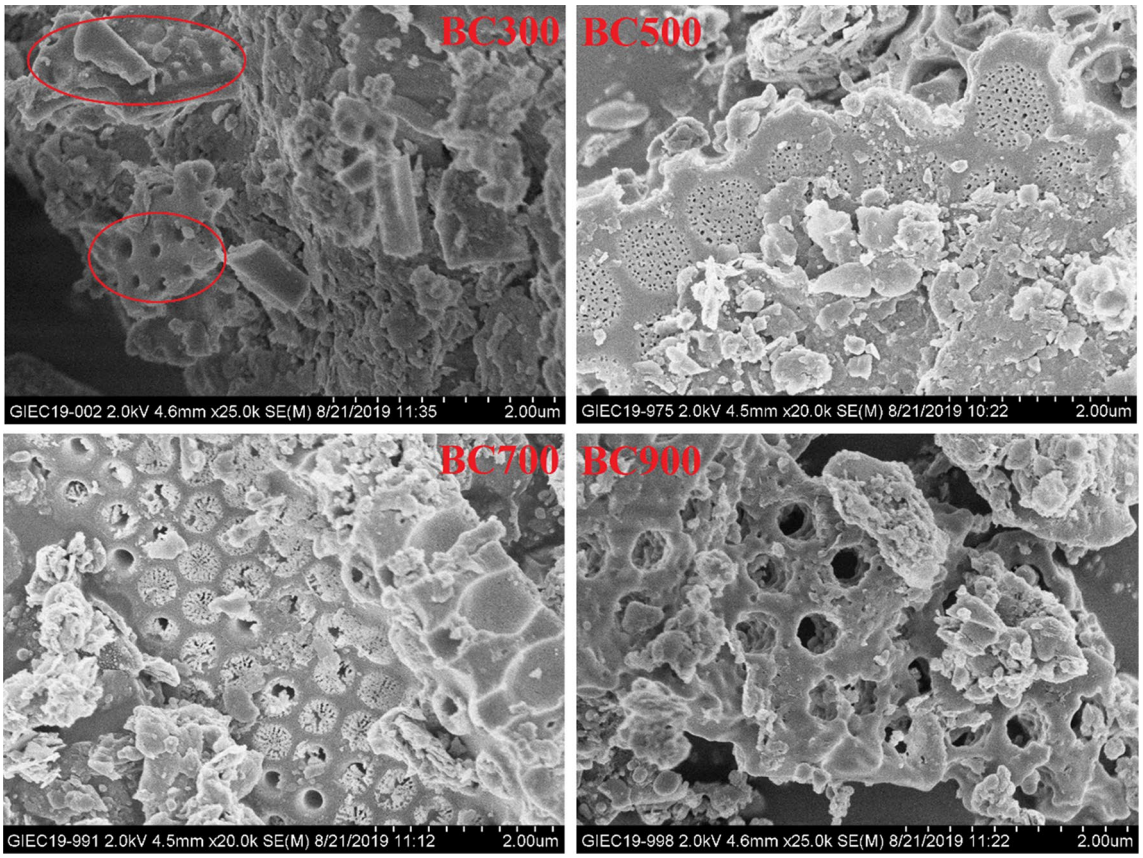

Fig. 3 Scanning electron microscopy images of biochar pyrolyzed at different temperatures

dewatering, carbon-based materials can remain porous, reducing the compressibility of sludge [8]. From SEM images of BC pyrolyzed at different temperatures (Fig. 3), we observed the pore structure characteristics of these complex materials. BC300 showed small voids and openings. Meanwhile, BC500 exhibited the sintering phenomenon, resulting in abundant pore structures; however, the surface of BC500 was uneven because the small blocks produced. In addition, the dimensions of the mesoporous pores were larger in BC900 than in BC700.

Sludge particles are generally considered to be negatively charged, and the existence of cations can break the relatively stable system, resulting in better sludge settling and dewatering performance [9]. Table 3 presents the elemental analysis and XRF results. Carbon, hydrogen, nitrogen, and sulfur showed the same trends; with increasing pyrolysis temperature, the contents decreased steadily. By contrast, contents of silicon, aluminum, calcium, potassium, and magnesium increased as the temperature increased. Finally, the titanium, zinc, copper, sodium, chlorine, and chromium contents remained relatively stable. The dominant inorganic elements in sludge pyrolyzed residue were sulfur, silicon, iron, aluminum, phosphorus, calcium, and potassium (Table 3).

The zeta potential represents the potential of the shear plane, which is an important index for characterizing the stability of colloidal dispersion. Peng et al. [19] also reported that zeta potential was related to dewatering. Higher absolute values of the zeta potential represent more stable systems, meaning that dissolution or dispersion can resist the aggregation of liquid, and tends to keep steady. The absolute values of the zeta potential of BC300, BC500, BC700, and BC900 were -22.17, -10.93, -18.57, and 4.61 mv, respectively (Table 3). Based on the general relationship between the zeta potential and system stability, the absolute values of zeta potential were less than 30 mv. In water and wastewater treatment technology, the zeta potential is used to study the optimal amount of coagulation and effect of coagulant. In general, good coagulation effects can be obtained at zeta potentials from ± 5 to 0 mV. And, zeta potential of WAS is -14.5 mv. The BC contains lots of soluble cation (Table 3), and they can neutralize the negative charge of activated wasted sludge. According to Table 3, soluble cations of BC500 are richer than others. Therefore, BC500 may have a better coagulation effect.

Table 3 Element content and zeta potential of BCs

Samples	O (%)	C (%)	H (%)	N (%)	S (%)	Si (%)	Fe (%)	Al (%)	P (%)	Ca (%)	K (%)	Mg (%)	Ti (%)	Zn (%)	Cu (%)	Na (%)	Cl (%)	Cr (%)	Zeta Potential (mV)
BC300	39.22	13.49	1.99	2.14	0.74	18.29	9.20	8.56	4.50	2.30	1.87	0.73	0.46	0.26	0.19	0.21	0.13	0.08	− 22.17
BC500	38.51	9.37	0.95	1.28	0.71	20.61	9.89	9.65	4.67	2.44	2.01	0.86	0.52	0.27	0.20	0.25	0.12	0.08	− 10.93
BC700	39.67	8.70	0.56	0.73	0.75	21.53	10.02	10.03	4.61	2.47	2.06	0.87	0.54	0.28	0.19	0.27	0.09	0.09	− 18.57
BC900	37.81	6.90	0.37	0.27	0.48	22.07	8.23	10.61	3.92	2.48	2.10	0.95	0.51	0.14	0.16	0.31	0.02	0.08	+4.61

Nitrogen adsorption

Water treatment is one of the main applications of mesoporous materials, as it can form water release channels and improve sludge dewaterability. Figure 4a shows the physical adsorption processes of the BC samples; the nitrogen physisorption isotherm curves proved the existence of mesoporous structures in the BC samples. Moreover, according to Fig. 4b, the pore sizes of the BC samples were mainly mesoporous, with few were macrospores. Surface area was calculated according to the BET method (43 points). Table 4 shows the variations of the pore properties of the BC samples. The BET surface area of BC300 was 14.32 $m^2\ g^{-1}$; when the pyrolysis temperature was increased to 900 °C, the surface area increased sharply to 57.48 $m^2\ g^{-1}$. High temperature is a positive influencing factor on surface area because of structural ordering and merging of pores [22, 28, 29]. The total pore volume increased slowly from BC300 to BC700, whereas BC900 had a slightly lower total pore volume (0.13 cc g^{-1}). The average pore size showed slight changes, except for BC500 (16.66 nm) and BC900 (9.35 nm). Combining BC surface characteristics with structural properties, we speculated that BC500 may have a better dewatering effect.

FTIR and XPS

Cationic groups (e.g., amino, ammonium, etc.) effectively enhance dewaterability [19]. The FTIR spectra (Fig. 5) and XPS spectra of carbon (Fig. 6) revealed abundant cationic groups in the BC samples. Moreover, cations can be used to neutralize negative charge in wastewater [30]. In the FTIR spectra (Fig. 5), several absorption bands were observed in the region from 3600 to 3000 cm^{-1}; they were related to C–H, N–H, and O–H bonds in organic compounds [17, 27, 31]. The peak at 2922 cm^{-1} corresponded to asymmetric aliphatic C–H groups and the peak at 2850 cm^{-1} was related to symmetric stretching vibration, both of which were assigned to fats and lipids in the sewage sludge [25, 32]. The characteristic wave numbers within 2400–2260 cm^{-1} represented CO_2 due to asymmetric stretching of its carbonyl group (C=O) [33]. The spectral bands of aldehydes and acids are within 1680–1780 cm^{-1} [30]. The peaks at 1653 and 1545 cm^{-1} were assigned to C=C stretching vibrations indicative of alkenes and the amide I bands of protein origin, respectively [27]. The remaining weak band at 1550–1700 cm^{-1} represented aromatic carbon vibrations as a unique characteristic of lignin. Bands representing $–CH_2–$, O–H, and $–CH_3$ were observed at 1459, 1425, and 1373 cm^{-1}, respectively [27]. The peak at 1330 cm^{-1} was assigned to O–H bending vibration and C=O stretching vibration. The remaining strong bands at 1035 and

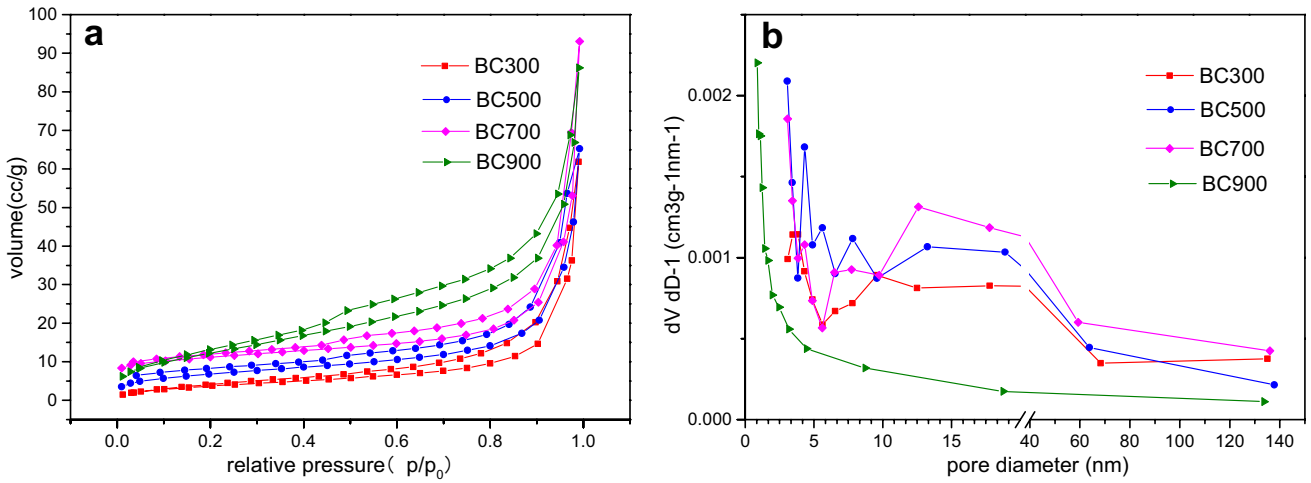

Fig. 4 **a** Nitrogen physisorption isotherms and **b** pore size distribution of the biochar samples

Table 4 Pore properties of the biochar samples

Samples	BC300	BC500	BC700	BC900
Surface area (m^2/g)	14.32	24.22	24.42	57.48
Total pore volume (cc/g)	0.096	0.106	0.146	0.136
Average pore size (nm)	26.70	16.66	23.49	9.35

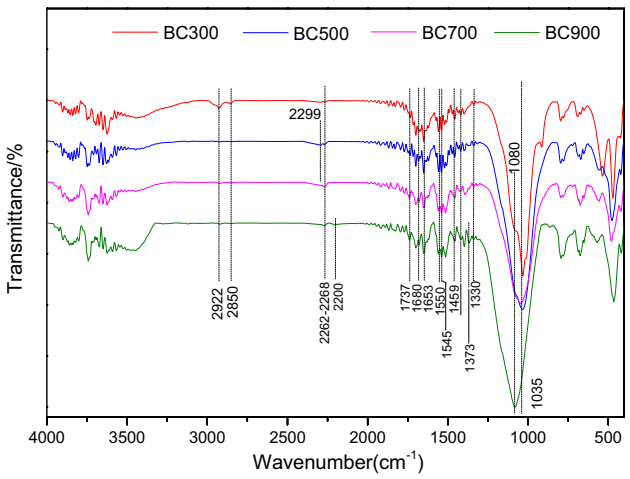

Fig. 5 Fourier-transform infrared spectra of the biochar samples

1080 cm^{-1}, representing C–O bonding, likely belonged to the cellulose structure [25, 31].

The total carbon content decreased with the increment of temperature (Table 3). However, the relative contents of C–C continuously increased from 55.87 to 75.76% from 300 to 900 °C (Fig. 6), as carbon skeleton structure. From 300 to 500 °C, the relative carbon of C=O decreased to 3.07%, after that C=O disappeared. We deduced that it related to organics like aldehyde, lipids, acids, and etc. [34]. C–N belonged to an N-containing heterocycles, with pyrolysis temperature increased, they thickened, and became more stable. C–O–Si/Al bridging bonds have excellent chemical stability [35], so it exist in BC300–BC900. Organometallic is corresponded to C=O, which is contained in carbon-containing metal salts. Generally, these materials have a high decomposition temperature and excellent stability, so this kind of bonds still were checked in BC900.

Evaluation of sludge dewaterability

Sewage sludge settling test

The curves of the V value revealed that a maximum average settlement rate of WAS was 5.6 mL min^{-1} in the first 10 min, after which the *V* value ultimately reached 18.5 mL, and then remained the same after 18 min (Fig. 7). Compared with WAS, the settlement rate of WAS added with BC accelerated significantly (Figs. 7, 8). The maximum average settlement rate reached 8.2 mL min^{-1} in the first 4 min, and the *V* value changed slightly after 6 min, and which ultimately reached 13 mL when WAS was added with BC500. Moreover, BC500 amendment yielded lower V values compared with MSWI fly ash and activated carbon, the settling time was within 10 min, and the efficiency of sludge gravity dewatering was significantly improved. Thus, SS added with BC500 exhibited the best settlement effect.

CST and dewatering by vacuum pump

Figure 9 shows the CSTs of the samples. The CST of WAS was 13.1 s, which reduced to 12.0 s with BC500 amendment and 11.6 s with BC700 amendment. These treatments yielded better results than the other BCs, coal fly ash, MSWI fly ash, and activated carbon. The moisture

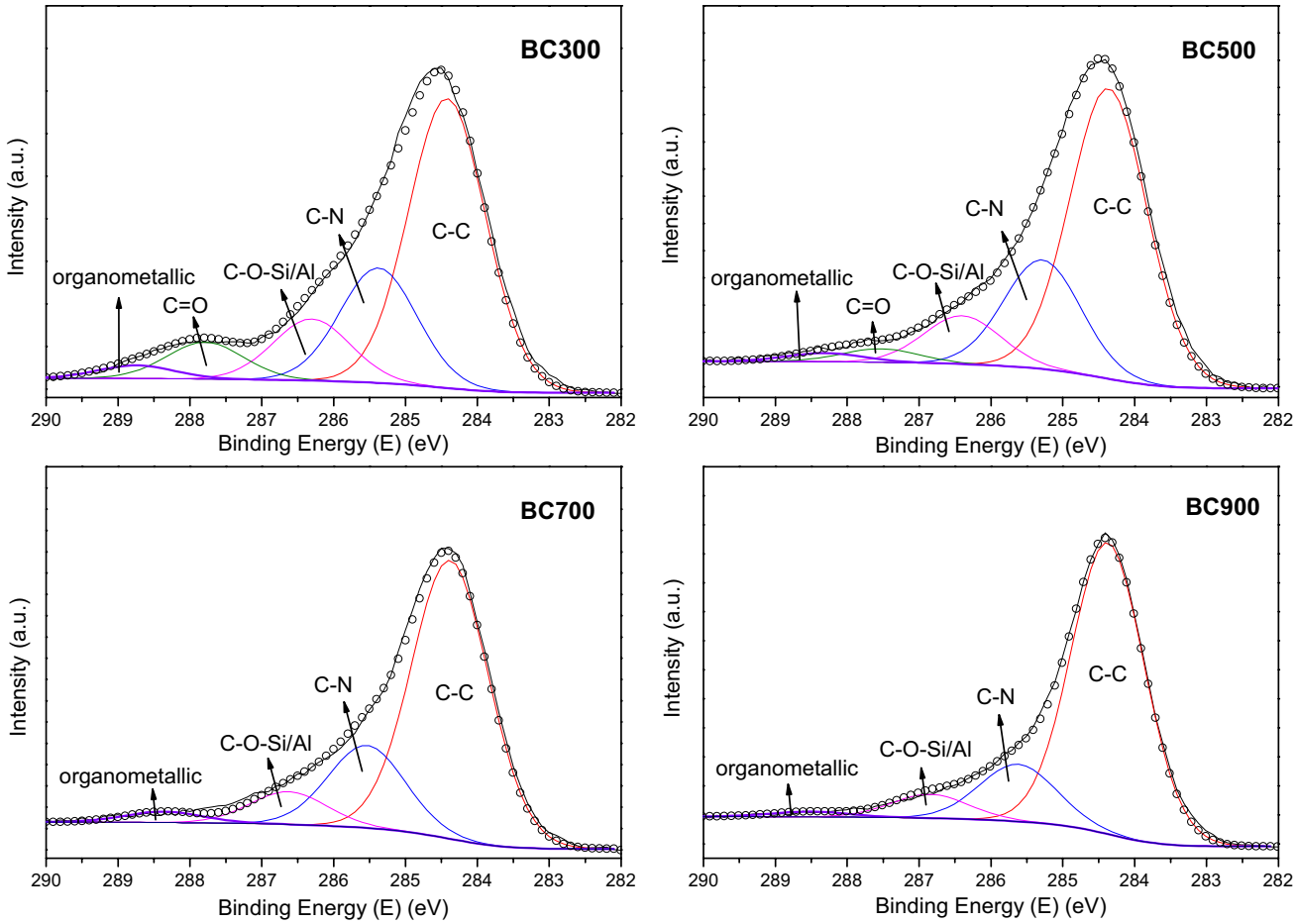

Fig. 6 C1s X-ray photoelectron spectroscopy spectra of the biochar samples

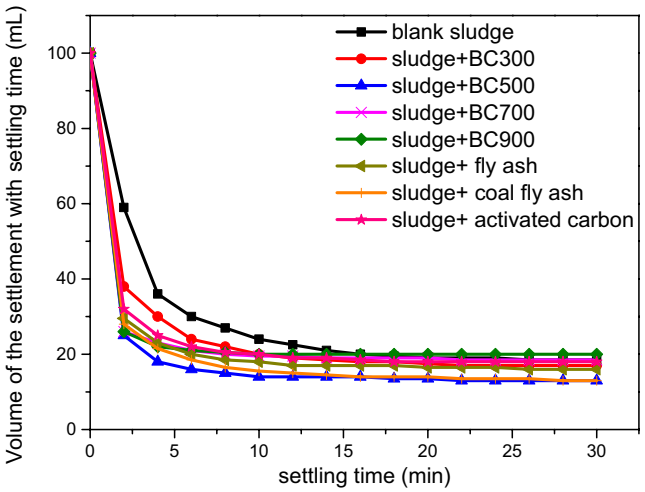

Fig. 7 Settlement curves of sewage sludge and sludge amended with coagulants

content of sewage sludge was 78.80%, all the sludge cake amendment with BC had low moisture content, and the sludge cake amendment with BC500 had the lowest value of 63.09%.

Combining the characteristics of sludge BC, the agglomerated grain size of BC500 was greater than that of BC700 (see BC SEM images in Fig. 3). Moreover, BC500 had a greater density of mesoporous pores with a diameter of 2–10 nm on the surface, whereas BC700 contained more mesoporous pores with a diameter > 10 nm (see Figs. 3 and 4b). Meanwhile, cationic groups improved WAS dewatering [19, 36]. In addition, the carbon contents decreased with increasing pyrolysis temperature (see Table 3), which could lead to changes of the organic functional groups in BC (see Fig. 6). Also, the BC samples contained high metal cation contents (see Table 3), which could achieve good dewatering effect, and neutralize negative charges in the wastewater treatment process. In addition, zeta potential is an important

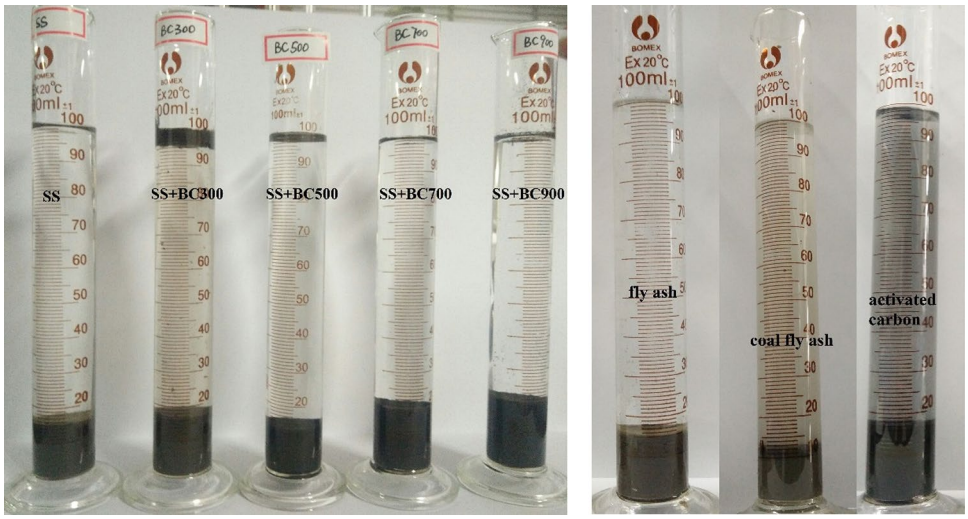

Fig. 8 Comparison of sludge sedimentation based on the sludge settling test after biochar amendment

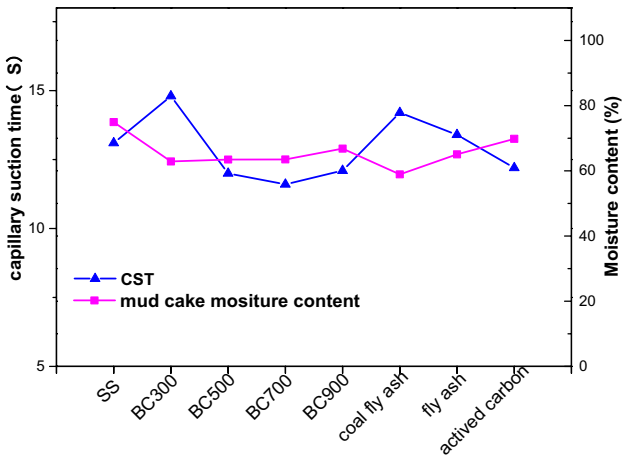

Fig. 9 Comparison of sludge sedimentation based on capillary suction time after biochar amendment

index to study the optimal amount of coagulation and the effect of the coagulant [37]. For BC500, although this sample did not have the maximum surface area, total pore volume, and average pore size, the zeta potential may have been influenced by the comprehensive effects of various factors, such as abundant pore structures, richer functional groups in BC500, high positive ion content, and surface charge. Overall, the comprehensive analysis of sludge dewatering performance using sewage sludge-derived BC indicated that BC500 yielded the optimal results.

Conclusion

BCs have well-developed structures, and are rich in soluble salts, negative surface charges, and organic functional groups. These characteristics are beneficial for reducing the sludge dewatering time. BC500 had the best sludge dewatering effect, which might relate to its rich pores with diameters 2–10 nm. Amendment of WAS with BC500 achieved a smaller settling volume 13 mL within 10 min, compared with the other BC samples, MSWI fly ash, coal fly ash, and activated carbon. In addition, both the CST and sludge cake moisture content of WAS added with BC500 were reduced 12 s and 63.5%. Thus, amendment of WAS with sewage sludge-derived BC, in particular that pyrolyzed at 500 °C, may improve sludge dewaterability.

Acknowledgements This work was supported by the National Key R&D Program of China [2018YFC1901200]; National Natural Science Foundation of China [51608507; 51676194]. We also thank the staff of Yanbu Municipal Wastewater Treatment Plant for experimental assistance.

Compliance with ethical standards

Conflict of interest The authors declare that they have no competing interest.

References

1. Thipkhunthod P, Meeyoo V, Rangsunvigit P, Rirksomboon T (2007) Describing sewage sludge pyrolysis kinetics by a combination of biomass fractions decomposition. J Anal Appl Pyrolysis 79:78–85. https://doi.org/10.1016/j.jaap.2006.10.005
2. Piippo S, Lauronen M, Postila H (2018) Greenhouse gas emissions from different sewage sludge treatment methods in north. J Clean Prod 177:483–492. https://doi.org/10.1016/j.jclepro.2017.12.232
3. Shi Y, Yang J, Yu W et al (2015) Synergetic conditioning of sewage sludge via Fe^{2+}/persulfate and skeleton builder: effect on sludge characteristics and dewaterability. Chem Eng J 270:572–581. https://doi.org/10.1016/j.cej.2015.01.122
4. Suopajärvi T, Liimatainen H, Hormi O, Niinimäki J (2013) Coagulation-flocculation treatment of municipal wastewater based on anionized nanocelluloses. Chem Eng J 231:59–67. https://doi.org/10.1016/j.cej.2013.07.010

5. Yang Z, Yuan B, Li H et al (2014) Amphoteric starch-based flocculants can flocculate different contaminants with even opposite surface charges from water through molecular structure control. Colloids Surf A Physicochem Eng Asp 455:28–35. https://doi.org/10.1016/j.colsurfa.2014.04.043
6. Hwa TJ, Jeyaseelan S (1997) Conditioning of oily sludges with municipal solid wastes incinerator fly ash. Water Sci Technol 35:231–238
7. Wu Y, Zhang P, Zeng G et al (2016) Enhancing sewage sludge dewaterability by a skeleton builder: biochar produced from sludge cake conditioned with rice husk flour and $FeCl_3$. ACS Sustain Chem Eng 4:5711–5717. https://doi.org/10.1021/acssuschemeng.6b01654
8. Thapa KB, Qi Y, Clayton SA, Hoadley AFA (2009) Lignite aided dewatering of digested sewage sludge. Water Res 43:623–634. https://doi.org/10.1016/j.watres.2008.11.005
9. Chen C, Zhang P, Zeng G et al (2010) Sewage sludge conditioning with coal fly ash modified by sulfuric acid. Chem Eng J 158:616–622. https://doi.org/10.1016/j.cej.2010.02.021
10. Yuan H, Lu T, Zhao D et al (2013) Influence of temperature on product distribution and biochar properties by municipal sludge pyrolysis. J Mater Cycles Waste Manag 15:357–361. https://doi.org/10.1007/s10163-013-0126-9
11. Lu T, Yuan H, Wang Y et al (2016) Characteristic of heavy metals in biochar derived from sewage sludge. J Mater Cycles Waste Manag 18:725–733. https://doi.org/10.1007/s10163-015-0366-y
12. Agrafioti E, Bouras G, Kalderis D, Diamadopoulos E (2013) Biochar production by sewage sludge pyrolysis. J Anal Appl Pyrolysis 101:72–78. https://doi.org/10.1016/j.jaap.2013.02.010
13. Yuan H, Lu T, Wang Y et al (2014) Influence of pyrolysis temperature and holding time on properties of biochar derived from medicinal herb (radix isatidis) residue and its effect on soil CO_2 emission. J Anal Appl Pyrolysis 110:277–284. https://doi.org/10.1016/j.jaap.2014.09.016
14. Méndez A, Terradillos M, Gascó G (2013) Physicochemical and agronomic properties of biochar from sewage sludge pyrolysed at different temperatures. J Anal Appl Pyrolysis 102:124–130. https://doi.org/10.1016/j.jaap.2013.03.006
15. Zhao B, O'Connor D, Zhang J et al (2017) Effect of pyrolysis temperature, heating rate, and residence time on rapeseed stem derived biochar. J Clean Prod 174:977–987. https://doi.org/10.1016/j.jclepro.2017.11.013
16. Wallace R, Seredych M, Zhang P, Bandosz TJ (2014) Municipal waste conversion to hydrogen sulfide adsorbents: investigation of the synergistic effects of sewage sludge/fish waste mixture. Chem Eng J 237:88–94. https://doi.org/10.1016/j.cej.2013.10.005
17. Zielińska A, Oleszczuk P, Charmas B et al (2015) Effect of sewage sludge properties on the biochar characteristic. J Anal Appl Pyrolysis 112:201–213. https://doi.org/10.1016/j.jaap.2015.01.025
18. Tan Z, Zou J, Zhang L, Huang Q (2018) Morphology, pore size distribution, and nutrient characteristics in biochars under different pyrolysis temperatures and atmospheres. J Mater Cycles Waste Manag 20:1036–1049. https://doi.org/10.1007/s10163-017-0666-5
19. Peng H, Zhong S, Xiang J et al (2017) Characterization and secondary sludge dewatering performance of a novel combined aluminum-ferrous-starch flocculant (CAFS). Chem Eng Sci 173:335–345. https://doi.org/10.1016/j.ces.2017.08.005
20. Sun Y, Zheng H, Zhai J et al (2014) Effects of surfactants on the improvement of sludge dewaterability using cationic flocculants. PLoS ONE 9:1–10. https://doi.org/10.1371/journal.pone.0111036
21. Yan M, Prabowo B, He L et al (2017) Effect of inorganic coagulant addition under hydrothermal treatment on the dewatering performance of excess sludge with various dewatering conditions. J Mater Cycles Waste Manag 19:1279–1287. https://doi.org/10.1007/s10163-016-0522-z
22. Onay O (2007) Influence of pyrolysis temperature and heating rate on the production of bio-oil and char from safflower seed by pyrolysis, using a well-swept fixed-bed reactor. Fuel Process Technol 88:523–531. https://doi.org/10.1016/j.fuproc.2007.01.001
23. Gascó G, Blanco CG, Guerrero F, Lázaro AMM (2005) The influence of organic matter on sewage sludge pyrolysis. J Anal Appl Pyrolysis 74:413–420. https://doi.org/10.1016/j.jaap.2004.08.007
24. Novak JM, Lima I, Xing B et al (2009) Characterization of designer biochar produced at different temperatures and their effects on a loamy sand. Ann Environ Sci 3:195–206
25. Gómez-Serrano V, Piriz-Almeida F, Durán-Valle CJ, Pastor-Villegas J (1999) Formation of oxygen structures by air activation. A study by FT-IR spectroscopy. Carbon N Y 37:1517–1528. https://doi.org/10.1016/S0008-6223(99)00025-1
26. Zhai Y, Peng W, Zeng G et al (2012) Pyrolysis characteristics and kinetics of sewage sludge for different sizes and heating rates. J Therm Anal Calorim 107:1015–1022. https://doi.org/10.1007/s10973-011-1644-0
27. De Oliveira Silva J, Filho GR, Da Silva Meireles C et al (2012) Thermal analysis and FTIR studies of sewage sludge produced in treatment plants. the case of sludge in the city of Uberlândia-MG, Brazil. Thermochim Acta 528:72–75
28. Kumar U, Maroufi S, Rajarao R et al (2017) Cleaner production of iron by using waste macadamia biomass as a carbon resource. J Clean Prod 158:218–224. https://doi.org/10.1016/j.jclepro.2017.04.115
29. Hung CY, Tsai WT, Chen JW et al (2017) Characterization of biochar prepared from biogas digestate. Waste Manag 66:53–60. https://doi.org/10.1016/j.wasman.2017.04.034
30. Pal S, Mal D, Singh RP (2005) Cationic starch: an effective flocculating agent. Carbohydr Polym 59:417–423. https://doi.org/10.1016/j.carbpol.2004.06.047
31. Grube M, Lin JG, Lee PH, Kokorevicha S (2006) Evaluation of sewage sludge-based compost by FT-IR spectroscopy. Geoderma 130:324–333. https://doi.org/10.1016/j.geoderma.2005.02.005
32. Gao N, Li J, Qi B et al (2014) Thermal analysis and products distribution of dried sewage sludge pyrolysis. J Anal Appl Pyrolysis 105:43–48. https://doi.org/10.1016/j.jaap.2013.10.002
33. Zhang J, Lü F, Zhang H et al (2015) Multiscale visualization of the structural and characteristic changes of sewage sludge biochar oriented towards potential agronomic and environmental implication. Sci Rep 5:1–8. https://doi.org/10.1038/srep09406
34. Rozada F, Otero M, Parra JB et al (2005) Producing adsorbents from sewage sludge and discarded tyres: characterization and utilization for the removal of pollutants from water. Chem Eng J 114:161–169. https://doi.org/10.1016/j.cej.2005.08.019
35. Dalchiele EA, Aurora A, Bernardini G et al (2005) XPS and electrochemical studies of ferrocene derivatives anchored on n- and p-Si(1 0 0) by Si–O or Si–C bonds. J Electroanal Chem 579:133–142. https://doi.org/10.1016/j.jelechem.2005.02.002
36. You L, Lu F, Li D et al (2009) Preparation and flocculation properties of cationic starch/chitosan crosslinking-copolymer. J Hazard Mater 172:38–45. https://doi.org/10.1016/j.jhazmat.2009.06.120
37. Wu Y, Zhang P, Zeng G et al (2017) Combined sludge conditioning of micro-disintegration, floc reconstruction and skeleton building ($KMnO_4$/$FeCl_3$/Biochar) for enhancement of waste activated sludge dewaterability. J Taiwan Inst Chem Eng 74:121–128. https://doi.org/10.1016/j.jtice.2017.02.004